A Rouse-tube model of dynamic rubber viscoelasticity

2007 J. Phys. A: Math. Theor. 40 14725

(http://iopscience.iop.org/1751-8121/40/49/008)

IOP PUBLISHING JOURNAL OF PHYSICS A: MATHEMATICAL AND THEORETICAL

J. Phys. A: Math. Theor. **40** (2007) 14725–14744 doi:10.1088/1751-8113/40/49/008

A Rouse-tube model of dynamic rubber viscoelasticity

W L Vandoolaeghe and E M Terentjev

Cavendish Laboratory, University of Cambridge, JJ Thomson Avenue, Cambridge CB3 0HE, UK

E-mail: wlv@physics.org

Received 21 August 2007, in final form 21 October 2007
Published 21 November 2007
Online at stacks.iop.org/JPhysA/40/14725

Abstract

The dynamic-mechanical response of a polymer network has been calculated using a stress-based Rouse model formalism. In contrast to the previous work, this improved formulation incorporates appropriate boundary conditions and provides a smooth crossover from the classical equilibrium result of rubber elasticity to the short time-scale relaxation. We develop a consistent implementation of the classical tube model, which is merged with the Rouse dynamics to take into account the entanglement effects. In a polymer network, crosslinks prevent the global reptation and constraint release. Entanglements thus acquire a different topological meaning and have a much stronger effect on the resulting mechanical response. We construct a dynamic stress tensor for a polymer network, which naturally covers the whole frequency/time range. Using this stress tensor, we first examine the equilibrium response to small shear and uniaxial deformations, and then investigate the linear dynamic response of a network for all the cases where the stress–tensor computations are analytically tractable.

PACS numbers: 61.41.+e, 83.80.Va, 83.80.Wx

1. Introduction

Understanding the molecular mechanisms of equilibrium and dynamic-mechanical response of polymer networks is counted amongst the most important unsolved problems in polymer physics. This is not surprising since polymer networks are highly complex disordered systems. An example of a macroscopic network polymer is rubber: it has a three-dimensional structure in which each chain is connected to all others by a sequence of junction points, called crosslinks. The resulting constraints, together with the conformational entropy arising from the chain flexibility, are responsible for rubber elasticity. This is the most basic view of a material that is expected to contain network inhomogeneities and other defects, e.g. trapped entanglements, which will alter its elastic behaviour as well.

The simplest theoretical models consider the network as being made of *phantom* or ideal chains. Each polymer is modelled by a three-dimensional random walk in space: chains may freely intersect and the network strand conformations are assumed to be independent of one another. To form a corresponding *phantom* network, the chains are linked to each other at their end points, but do not interact otherwise. In particular, they are able to fluctuate freely between crosslinks. In a real network, the exact location of the crosslinks can vary from one specimen to the next. However, any two samples having different crosslink realizations will exhibit similar macroscopic properties. The phantom model, although crude, is the customary first approach when solving polymer theory problems.

Attempting to improve the phantom model, one is faced with the complexity of entanglements and their topological constraints. Modern understanding of network or *rubber* elasticity has come a long way since the first molecular models were developed in the 1930s [1]. Recent classic equilibrium theories are sophisticated and try to incorporate topological constraints from crosslinks and entanglements, excluded volume effects and network features such as dangling ends, inhomogeneities and noninteracting strands [2–5], and even thermal elastic fluctuations [6]. Although generally successful and certainly valid conceptually, existing theories do not provide a fully adequate understanding of rubber elasticity. Predicted stress–strain relationships and elastic moduli under various non-trivial types of deformation still show discrepancies with experiment. However, it is general *dynamic* response theories for polymer networks that are deficient and markedly less successful than the plethora of equilibrium (long time limit) models that currently exist. Although there is a large body of seminal literature covering the area of dynamics of *uncrosslinked* polymer chains (melts and solutions) [7–10], corresponding investigations into the dynamics and relaxation of fully percolating random networks are still lacking.

The dynamic response of networks is an important research area and plays a role in areas as diverse as vibration damping and the toughening of biological tissues [11]. Fundamental polymer theory research provides a backbone for investigating and predicting properties of these systems. An extension of the tube-model theory for rubbers, first proposed by Edwards [12], was based on the reptation theory [13, 14]. Few theories go beyond the phenomenological level to try and link macroscopic properties of the system with a molecular structure. One of the first attempts to derive a statistical dynamics of networks by employing a viscosity coefficient, as in the Rouse model, never managed to explain the full set of dynamic properties [16]. A tube model approach [17] has been used to analyse the relaxation of flexible network strands between crosslink points and to obtain the linear complex modulus of a highly entangled rubbery network, though it was limited to the small frequency range only.

More recently a stress–tensor formulation [18], based on the Rouse mode expansion, was used to look at the linear dynamic response over the *whole* frequency range. The motivation behind the work was to find an analytical method for investigating polymer network dynamics and laying a foundation for future investigations. The stress–tensor approach naturally allowed an analytical description of the relaxation of an affinely deformed ideal network over the whole time range. Although such an entropic theory alone was not wholly satisfactory (for example, to examine glassy dynamics in a short time limit), it remained a self-consistent and interesting model to start with. Although quite successful for a phantom model, it was clear that the stress–tensor model [18] could still be improved in many ways. First, it did not incorporate appropriate boundary conditions for the crosslinks, which led to unfamiliar rubber elasticity behaviour in the long time limit when the classic behaviour was expected. In section 2 we review the improved phantom model [19], which employs more robust boundary conditions. Second, it is necessary to incorporate the required level of complexity by accounting for entanglement constraints. In section 3, by expanding on the phantom stress–tensor approach

and employing ideas from an existing tube model for rubber elasticity [20, 21], we construct a Rouse-tube model of rubber viscoelasticity. The merit of the present constrained dynamic Rouse model lies in that it is the first model to naturally cover the equilibrium *and* dynamic-relaxation ranges of an *entangled* network response. In section 3.3, we calculate the stress tensor for small shear and uniaxial deformations in the long time limit. Lastly, in section 3.4, we investigate different regimes of tube and segment relaxations, and obtain the associated shear moduli. In this way, we highlight the tractable areas within the tube model approach and separate it from more challenging areas for future research.

2. Constrained phantom network model

Before considering entangled rubber, we shall review the results of the earlier phantom chain network theory, which provides the basic building blocks for all future network stress–tensor approaches.

2.1. Constrained Rouse dynamics

The dynamics of a single ideal chain is traditionally described by the Rouse model of beads, each connected to its nearest neighbour with Gaussian springs. In a solution, ideal Rouse chains obey the following stochastic partial distribution equation for the position of a chain segment $\boldsymbol{r}_n(t)$:

$$\zeta \dot{\boldsymbol{r}}_n = -\kappa(2\boldsymbol{r}_n - \boldsymbol{r}_{n+1} - \boldsymbol{r}_{n-1}) + \boldsymbol{f}_n \longrightarrow \zeta \frac{\mathrm{d}\boldsymbol{r}_n}{\mathrm{d}t} = \kappa \frac{\partial^2 \boldsymbol{r}_n}{\partial n^2} + \boldsymbol{f}_n, \tag{1}$$

where $\kappa \equiv 3k_{\mathrm{B}}T/\ell^2$ is the spring constant, ζ is the viscous drag coefficient on each segment and $\boldsymbol{f}_n$ is the (thermal) white noise due to random collisions with the environment. The dynamics of the whole chain can be described by a set of normal modes. For a free chain, the elastic forces vanish at the ends and leads to the classical Rouse formalism as described in e.g. [7]. However, in a network the chain ends are crosslinked and thus constrained to a certain extent. If we consider them to be completely fixed, such that a force can propagate from each end, the symmetric boundary conditions are

$$\boldsymbol{r}_{n=0} = 0 \qquad \text{and} \qquad \boldsymbol{r}_{n=N} = \boldsymbol{R}. \tag{2}$$

It is important to emphasize the need for the force on the end segments, $\kappa \partial \boldsymbol{r}_n/\partial n|_{n=0,N}$, to be non-zero. There are, perhaps surprisingly, only few examples in the literature where Rouse modes have been derived for boundary conditions other than free ends. They include the analysis for ends fixed at the same point (a loop with $\boldsymbol{r}_n = \boldsymbol{r}_0 = \boldsymbol{0}$) [22], for one end fixed and one free (a tethered chain) [23, 24], and for a block copolymer system with free ends, but chain connectivity at the interblock junction [25]. Here, we need to find the independent normal modes, $\{\boldsymbol{x}_p(t)\}$, of the constrained Rouse chain, such that the boundary conditions (2) are satisfied. We therefore consider a linear transformation of $\{\boldsymbol{r}_n(t)\}$: $\boldsymbol{x}_p = \int_0^N \mathrm{d}n\, \boldsymbol{r}_n(t)\phi_{pn}$. Moreover, we want the equation of motion (1) to transform to one that represents the Brownian motion of decoupled oscillators. The general solution of the type $\phi_{pn} = c_1 \cos b_p n + c_2 \sin b_p n$—such that ϕ_{pn} stays a periodic function—cannot satisfy the fixed-position boundary conditions, whilst having non-zero forces at the ends. The key to finding the constrained Rouse modes is to factor out the $\boldsymbol{R}$ dependence, such that the position vectors of the Rouse segments can be written as follows: $\boldsymbol{r}_n(t) = \mathfrak{g}(n, \boldsymbol{R}) + \boldsymbol{\rho}_n(t)$, such that $\boldsymbol{\rho}_n(t)$ describes a loop with ends fixed at the same point, $\boldsymbol{\rho}_0 = \boldsymbol{\rho}_N = \boldsymbol{0}$. Finally, in order to satisfy (2), we impose the following constraint on the time-independent part of

$\boldsymbol{r}_n$: $\mathfrak{g}(0, \boldsymbol{R}) = 0$ and $\mathfrak{g}(N, \boldsymbol{R}) = \boldsymbol{R}$. The function $\mathfrak{g}$, which satisfies (2), is not unique, but the simplest is linear in n, that is, $\mathfrak{g}(n, \boldsymbol{R}) = n(\boldsymbol{R}/N)$. We thus have the following modified Rouse mode expansion for spatially constrained chain ends:

$$\boldsymbol{r}_n(t) = n\left(\frac{\boldsymbol{R}}{N}\right) + \underbrace{2\sum_{p=1}^{N} \mathrm{x}_p(t)\sin\left[\frac{p\pi n}{N}\right]}_{\equiv\, \boldsymbol{\rho}_n(t)}, \tag{3a}$$

and

$$\mathrm{x}_p(t) \equiv \frac{1}{N}\int_0^N \mathrm{d}n\,\boldsymbol{\rho}_n(t)\sin\left[\frac{p\pi n}{N}\right], \tag{3b}$$

and the normal modes $\boldsymbol{x}_p$ transform the Langevin equation (1) to a set of decoupled Rouse equations:

$$\zeta_\mathrm{R}\frac{\mathrm{d}\mathbf{x}_p}{\mathrm{d}t} = -k_p\mathbf{x}_p + \hat{\boldsymbol{f}}_p, \qquad \text{where} \quad \zeta_\mathrm{R} = 2N\zeta, \tag{4}$$

and the associated stochastic force has the following statistical properties: $\langle \hat{f}_{p\alpha}(t)\hat{f}_{q\beta}(t')\rangle = 2\zeta_\mathrm{R}k_\mathrm{B}T\delta_{pq}\delta_{\alpha\beta}\delta(t-t')$ and $\langle \hat{f}_{p\alpha}(t)\rangle = 0$. As usual, this is a diffusion problem for an effective 'particle' in a harmonic potential with a constant

$$k_p = \frac{2\pi\kappa p^2}{N} = \frac{6\pi^2 k_\mathrm{B}T}{N\ell^2}p^2. \tag{5}$$

The forces at the end points are proportional to $\dot{\boldsymbol{r}}_n = \boldsymbol{R}/N + 2\sum_p(-1)^p\boldsymbol{x}_p p\pi/N$.

The microscopic stress tensor $\sigma_{\alpha\beta}$ of a viscoelastic material consists of the stress contribution due to the polymers, the solvent molecules and an isotropic pressure term $\sim k_\mathrm{B}T\delta_{\alpha\beta}$. The last two contributions are not important for an incompressible elastomer and are thus neglected from here onwards [7]. In the Rouse model the polymeric contribution to the stress is given by the following tangent correlation function, in the continuous limit,

$$\sigma^{(p)}_{\alpha\beta} = \frac{c}{N}\kappa\int_0^N \mathrm{d}n\left\langle\frac{\partial r_{n\alpha}}{\partial n}\frac{\partial r_{n\beta}}{\partial n}\right\rangle_\psi, \tag{6}$$

where c is the monomer density, N is the number of segments of a given polymer chain, so that $\tilde{c} \equiv c/N$ is the number of chains per unit volume in the system proportional to the crosslink density. The average $\langle\cdots\rangle_\psi$ denotes the time average of the components of stochastic force $\hat{\boldsymbol{f}}_p(t)$ over the distribution

$$\psi[\hat{f}_{p\alpha}(t)] \propto \exp\left(-\frac{1}{4\zeta_\mathrm{R}k_\mathrm{B}T}\int \mathrm{d}t\,\hat{f}_{p\alpha}(t)^2\right). \tag{7}$$

The microscopic stress tensor of a single constrained polymer chain is found by substituting (3a) into the stress expression (6):

$$\sigma^{(p)}_{\alpha\beta} = \frac{c}{N}k\int_0^N \mathrm{d}n\left(\frac{\langle R_\alpha R_\beta\rangle}{N^2} + \left\langle\frac{R_\alpha}{N}\frac{\partial\rho_{n\beta}}{\partial n}\right\rangle + \left\langle\frac{\partial\rho_{n\alpha}}{\partial n}\frac{R_\beta}{N}\right\rangle + \left\langle\frac{\partial\rho_{n\alpha}}{\partial n}\frac{\partial\rho_{n\beta}}{\partial n}\right\rangle\right). \tag{8}$$

The second and third terms above are zero, since $\int_0^N \mathrm{d}n(\partial\rho_{n\alpha})/(\partial n) = 0$. In terms of normal modes, the stress tensor of a single chain is thus given by

$$\sigma^{(p)}_{\alpha\beta} = \frac{ck}{N^2}\langle R_\alpha R_\beta\rangle + \frac{c}{N}\sum_p k_p\langle x_{p\alpha}(t)x_{p\beta}(t)\rangle_\psi. \tag{9}$$

2.2. *Stress tensor for a phantom network*

Now consider a random network of constrained, end-linked chains, deformed by a strain tensor $\boldsymbol{E}$. For a phantom network model the end-to-end vectors of each network strand transform affinely, $\boldsymbol{R} = \boldsymbol{E} \cdot \boldsymbol{R}_0$, and the stress tensor in (9) is quenched averaged over the isotropic Gaussian distribution:

$$\sigma_{\mathrm{netw},\alpha\beta} = \left[\sigma^{(p)}_{\alpha\beta}\right]_{\mathbb{P}(\boldsymbol{R}_0)} \tag{10a}$$

$$= \frac{ck}{N^2}[(\boldsymbol{E}\cdot\boldsymbol{R}_0)_\alpha(\boldsymbol{E}\cdot\boldsymbol{R}_0)_\beta]_{\mathbb{P}(\boldsymbol{R}_0)} + \frac{c}{N}\sum_p k_p \langle x_{p\alpha}(t)x_{p\beta}(t)\rangle_\psi \tag{10b}$$

$$= \frac{c}{N}k_\mathrm{B}T(\boldsymbol{E}\boldsymbol{E}^\top)_{\alpha\beta} + \frac{c}{N}\sum_p k_p \langle x_{p\alpha}(t)x_{p\beta}(t)\rangle_\psi . \tag{10c}$$

The notation $[\cdots]_\mathbb{P}$ refers to the quenched average over the most convenient and appropriate probability distribution $\mathbb{P}(\boldsymbol{R}_0)$ of the end-to-end vectors, given by

$$\mathbb{P}(\boldsymbol{R}_0) = \left(\frac{3}{2\pi N\ell^2}\right)^{\frac{3}{2}} \exp\left(-\frac{3\boldsymbol{R}_0^2}{2N\ell^2}\right). \tag{11}$$

In order to investigate the entire time spectrum of the dynamic-mechanical response, we need to use the full solution of the Langevin equation (4):

$$x_{p\alpha}(t) = x_{p\alpha}(0)\,\mathrm{e}^{-t/\tau_p} + \frac{1}{\zeta_\mathrm{R}}\int_0^t \mathrm{e}^{-(t-t')/\tau_p}\,\hat{f}_{p\alpha}(t')\,\mathrm{d}t', \tag{12}$$

describing the normal modes and depending explicitly on the initial condition. From the Langevin equation (4), one finds the time-correlation functions of the normal modes. In equilibrium, they are given by

$$\langle x_{p\alpha}(t)x_{q\beta}(0)\rangle_{\psi[f]} = \delta_{pq}\delta_{\alpha\beta}\frac{k_\mathrm{B}T}{k_p}\,\mathrm{e}^{-t/\tau_p}, \tag{13}$$

where $\tau_p = \zeta_\mathrm{R}/k_p \equiv \tau_\mathrm{R}/p^2$ is the relaxation time of the pth Rouse mode. The classical Rouse time for a chain of N segments represents the relaxation time of the longest ($p = 1$) mode; $\tau_\mathrm{R} = \zeta N^2\ell^2/(3\pi^2 k_\mathrm{B}T)$ [7]. In (10*b*) we imposed the constraint that only the topologically quenched crosslinks are affected by the deformation, thereby applying the affine deformation approximation only to the span vectors $\boldsymbol{R}$. Here, at an arbitrarily short time after an instantaneous strain, we assume that the positions of *all* the segments between two crosslinks are changed on instantaneous deformation, in the same proportion as the macroscopic strain dictates. We choose an appropriate initial condition $x_{p\alpha}(0)$, by distinguishing between the state of each segment *just* before the strain $\boldsymbol{E}$ is imposed on the material, at $t = 0^-$, and just after $\boldsymbol{E}$ is applied, $t = 0^+$. Thus, applying a step strain $\boldsymbol{E}$ at time $t = 0$, a given segment position before deformation $\boldsymbol{r}_n(0^-)$ will change to $\boldsymbol{r}_n(0^+)$ *after* deformation:

$$\boldsymbol{r}_n(0^+) = \boldsymbol{E}\cdot\boldsymbol{r}_n(0^-) \quad \longrightarrow \quad \boldsymbol{x}_p(0^+) = \boldsymbol{E}\cdot\boldsymbol{x}_p(0^-). \tag{14}$$

Applying the affine deformation to all normal modes, the full solution of the Langevin equation, given by (12), becomes

$$x_{p\alpha}(t) = E_{\alpha\mu}x_{p\mu}(0^-)\,\mathrm{e}^{-t/\tau_p} + \frac{1}{\zeta_\mathrm{R}}\int_0^t \mathrm{e}^{-(t-t')/\tau_p}\,\hat{f}_{p\alpha}(t')\,\mathrm{d}t'. \tag{15}$$

After substituting this $x_{p\alpha}(t)$ the correlation function in (10) can thus be written as follows, to illustrate the $\boldsymbol{E}$-dependence:

$$\begin{aligned}\langle x_{p\alpha}(t)x_{p\beta}(t)\rangle_\psi = &\left\langle E_{\alpha\mu}E_{\beta\eta}\overbrace{x_{p\mu}(0^-)x_{p\eta}(0^-)}^{\delta_{\mu\eta}\frac{k_\mathrm{B}T}{k_p}}\,\mathrm{e}^{-2t/\tau_p}\right\rangle_\psi \\ &+ E_{\alpha\mu}x_{p\mu}(0^-)\,\mathrm{e}^{-t/\tau_p}\frac{1}{\zeta_\mathrm{R}}\int_0^t \mathrm{d}t'\,\mathrm{e}^{-(t-t')/\tau_p}\langle f_{p\beta}(t')\rangle_\psi \\ &+ E_{\beta\eta}x_{p\eta}(0^-)\,\mathrm{e}^{-t/\tau_p}\frac{1}{\zeta_\mathrm{R}}\int_0^t \mathrm{d}t'\,\mathrm{e}^{-(t-t')/\tau_p}\langle f_{p\alpha}(t')\rangle_\psi \\ &+ \frac{1}{\zeta_\mathrm{R}^2}\int_0^t \mathrm{d}x\int_0^t \mathrm{d}y\,\mathrm{e}^{-(2t-x-y)/\tau_p}\langle f_{p\alpha}(x)f_{p\beta}(y)\rangle_\psi, \end{aligned} \tag{16}$$

where $\langle\cdots\rangle_\psi$ denotes the time average over the functional distribution $\psi[\hat{\boldsymbol{f}}_p(t)]$, defined in (7). The cross terms vanish since $\langle f_{n\alpha}(t)\rangle_\psi = 0$, and $\langle \hat{f}_{p\alpha}(t)\hat{f}_{q\beta}(t')\rangle = 2\zeta_\mathrm{R}k_\mathrm{B}T\delta_{pq}\delta_{\alpha\beta}\delta(t-t')$, leads to a constant last term. Completing all the integrations with respect to time, we obtain

$$\langle x_{p\alpha}(t)x_{p\beta}(t)\rangle_\psi = E_{\alpha\eta}E_{\beta\eta}\frac{k_\mathrm{B}T}{k_p}\,\mathrm{e}^{-2t/\tau_p} + \frac{k_\mathrm{B}T}{k_p}(1+\mathrm{e}^{-2t/\tau_p})\delta_{\alpha\beta}. \tag{17}$$

Substituting this back into (10*c*), we obtain the complete network stress tensor,

$$\sigma_{\mathrm{netw},\alpha\beta} = \frac{c}{N}k_\mathrm{B}T\left\{(\boldsymbol{E}\boldsymbol{E}^\top)_{\alpha\beta}\left(1+\sum_{p=1}^{N}\mathrm{e}^{-2t/\tau_p}\right)+\sum_{p=1}^{N}(1-\mathrm{e}^{-2t/\tau_p})\delta_{\alpha\beta}\right\}. \tag{18}$$

Note that this stress tensor contains an isotropic (time-dependent) term which is a contribution to an effective pressure, which is irrelevant unless we need to examine the small effects of changing volume at constant pressure in an open network [26].

Let us first consider an isovolumetric uniaxial deformation, with the sample instantaneously stretched in the z-direction by a factor λ, that is, $E_{zz} = \lambda$, $E_{xx} = E_{yy} = \lambda^{-1/2}$, $E_{\alpha\neq\beta} = 0$. In this geometry, the diagonal components σ_{xx} and σ_{yy} are equal. The response is characterized by the stress difference, called the tensile stress:

$$\sigma_\mathrm{T} = \sigma_{zz} - \sigma_{xx} = \frac{c}{N}k_\mathrm{B}T\left(\lambda^2-\frac{1}{\lambda}\right)\left(1+\sum_{p=1}^{N}\mathrm{e}^{-2t/\tau_p}\right), \tag{19}$$

which directly follows from (18). Seminal literature mentions that it is important to examine relative stress expressions only, cf [27]. Since additional pressure terms arise due to a small change in the volume of the network during deformation, correct stress expressions could also be obtained by means of volume relaxation calculations, cf [26, 28]. The resulting shear modulus takes the form

$$G(t) = G_0\left(1+\sum_{p=1}^{N}\mathrm{e}^{-2t/\tau_p}\right), \qquad \text{with} \quad G_0 = \tilde{c}k_\mathrm{B}T, \tag{20}$$

where $\tilde{c} = c/N$ is proportional to the crosslinking density. At small extensions, $\lambda \to 1+\varepsilon$, we trivially verify that the Young modulus $Y(t) \equiv \sigma/\varepsilon = 3G(t)$. In the equilibrium limit ($t \to \infty$) the relaxation of all Rouse modes is complete, and the material returns to the rubber elastic behaviour of a classical phantom network, $G(t) \to G_0$. In the short time limit ($t \to 0$), $G \to NG_0$, akin to the 'glassy' plateau. In this limit, no long-range relaxations can take place and the effective spring constants between neighbouring segments are thus probed, which give

the modulus N times higher. Between these two limits, as the time of relaxation increases, more and more Rouse modes become relevant channels for stress relaxation. The formulation provides a smooth crossover in accounting for the dynamical behaviour spanning all timescales. It is customary to consider the dynamic shear modulus, $G^*(\omega) = \mathrm{i}\omega \int_{-\infty}^{\infty} \mathrm{d}t\, \mathrm{e}^{-\mathrm{i}\omega t} G(t)$, when investigating stress relaxation. In [19] the key properties of $G^*(\omega)$ are summarized and the results of the calculation are compared with both the classical phantom network approach in equilibrium [15] and the dynamic elongation experiments. Although a simple phantom model, it captures the qualitative features of stress relaxation in networks [29] and some of the quantitative aspects, such as the exponents seen in the dynamic modulus.

3. Constrained Rouse-tube network model

So far we have applied the classic Rouse model to a phantom network: hydrodynamic interactions and topological effects were ignored, with the environment only producing friction without affecting the chain conformations. A necessary improvement would be to include trapped entanglements and excluded volume effects into the stress–tensor approach.

3.1. Reptation theory of rubbery networks

There are many free energy models that investigate rubber elasticity and also include topological constraints, but most are not suited for dynamics calculations. However, the techniques developed to describe the tube model [20, 21], inspired by the original ideas of Edwards [30], are transferable to dynamics. It effectively assumes that each network strand is limited in its lateral fluctuations by the presence of neighbouring chains. Therefore, each segment of a polymer only explores configurations in a limited, tube-like volume, which is much smaller than the space occupied by a phantom chain. One can imagine the whole strand fluctuating around a certain mean trajectory, which is called the primitive path in the classic reptation theory [30]. The primitive path can be considered as a random walk with an associated typical step length, which is much bigger than the polymer step length, as shown in figure 1. The number of tube segments M is determined by the average number of entanglements per chain, such that an unentangled chain corresponds to $M = 1$. Note that all the chains are in constant thermal motion, altering the local constraints they impose on each other. Hence, the fixed tube is a gross simplification of the real situation. However, one expects this to be an even better approximation in rubber than in a corresponding melt (where the success of the reptation theory is undeniable), because the restriction on chain reptation diffusion in a crosslinked network prohibits constraint release [21, 31].

Along one network strand consisting of N segments of effective step length ℓ, there are M tube segments, each containing $s_m, m = 1, \ldots, M$, monomer steps. Since the strand is permanently crosslinked, the number of segments is conserved:

$$\sum_{m=1}^{M} s_m = N. \tag{21}$$

There are effectively two random walks, with both having the same end-to-end vector $\boldsymbol{R}_0$, between the connected crosslinking points. The first is the topologically fixed primitive path, shown as solid black vector lines in figure 1; the second is the polymer chain restricted to move around it, depicted as a dashed bead-spring chain. The number M of tube segments (also called the nodes of the primitive path) is a free parameter of the theory, dependent on the length of each polymer strand and the entanglement density. Each tube segment m can be

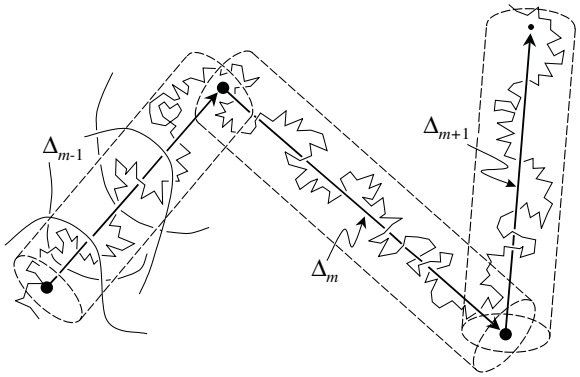

Figure 1. A polymer strand is surrounded by neighbouring chains, which effectively confine the strand to a tube. The tube segment m, with the span vector Δ_m along its axis, contains s_m monomer steps, where m runs from 1 to M.

described by the span vector $\boldsymbol{\Delta}_m$, joining the equilibrium positions of the strand monomers at the two ends of each tube segment.

Since the primitive path is a topologically frozen characteristic of each network strand, we shall assume that all span vectors $\boldsymbol{\Delta}_m$ deform affinely with the macroscopic strain: $\boldsymbol{\Delta}'_m = \boldsymbol{E} \cdot \boldsymbol{\Delta}_m$. This is the central point in the model: the rubber elastic response arises due to the change in the number of polymer configurations in a distorted primitive path. Next, the number of conformations is evaluated by separately looking at chain excursions parallel and perpendicular to the tube axis, along each span $\boldsymbol{\Delta}_m$. The earlier work [20, 26] gives the details of this evaluation, which gives the product of the statistical weights of parallel and perpendicular excursions of a polymer segment consisting of s_m monomers in a tube segment of span $\boldsymbol{\Delta}_m$:

$$\mathbb{W}_m = W_m^{\parallel} W_m^{\perp} \propto \frac{1}{\sqrt{s_m}} \exp\left(-\frac{3}{2\ell^2 s_m}\boldsymbol{\Delta}_m^2 - \frac{1}{3}q_0 \ell s_m\right), \tag{22}$$

where q_0 is a parameter determining the strength of the confining potential and thus related to the tube diameter, cf [3, 12, 26]. Therefore, the full number of configurations of the whole strand is given by

$$\mathbb{W} = \int_0^N \mathrm{d}s_1 \cdots \int_0^N \mathrm{d}s_M \left(\prod_{m=1}^{M} \mathbb{W}_m\right) \delta\left(\sum_{m=1}^{M} s_m - N\right), \tag{23}$$

where the constraint (21) on the polymer contour length between two crosslinks is implemented by the delta-function. The statistical summation in (23) takes into account the reptation motion of the polymer between its two crosslinked ends, changing the number of segments constrained within each tube segment and finally equilibrating for a given conformation of the primitive path.

By rewriting the delta-function as $\delta(x) = \frac{1}{2\pi}\int \mathrm{d}k\, \mathrm{e}^{\mathrm{i}kx}$, one can find the saddle points s_m^* which make the exponent of the statistical sum (23) stationary. The integrals over s_m and the auxiliary variable k are both approximated by means of the steepest descent method. Consequently, the equilibrium number of polymer segments confined within a tube segment with the span vector $\boldsymbol{\Delta}_m$ is given by

$$\overline{s}_m = \frac{N\Delta_m}{\sum_{m=1}^{M}\Delta_m}, \tag{24}$$

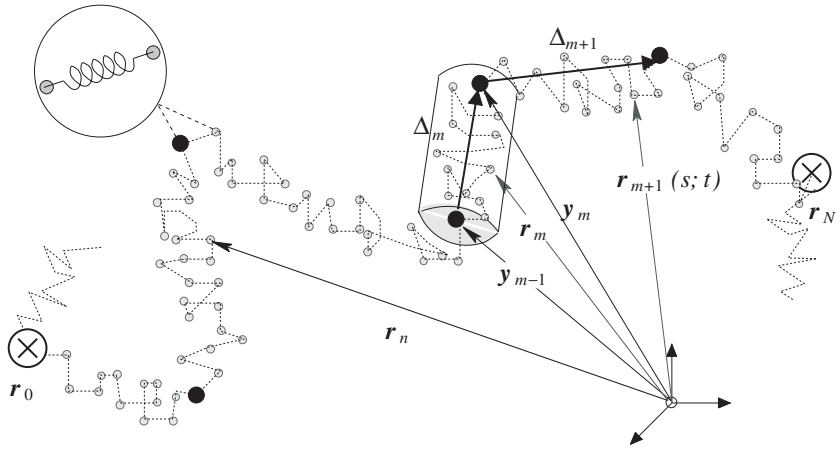

Figure 2. A polymer strand between crosslinks (⊗), confined by M tube segments (only the tube of segment m is explicitly shown here). A tube segment m, with the span vector $\Delta_m = \boldsymbol{y}_m - \boldsymbol{y}_{m-1}$ along its axis, contains s_m monomer steps. The nth monomer has position vector $\boldsymbol{r}_n$. The end-to-end vector of the polymer strand is $\boldsymbol{R} = \boldsymbol{r}_N - \boldsymbol{r}_0$. In the tube model, we denote the position vector of a monomer segment by $\boldsymbol{r}_m(s,t)$, cf (28).

where $\Delta_m = |\boldsymbol{\Delta}_m|$ is the length of the mth step of the primitive path. After integrating out the freedom in the distribution of $\{s_m\}$ in this way, the *total* number W of configurations of one strand, confined within a tube whose primitive path is described by the set of vectors $\{\boldsymbol{\Delta}_m\}$, is proportional to the probability distribution:

$$W(\boldsymbol{\Delta}_1, \ldots, \boldsymbol{\Delta}_M) \propto \mathbb{P}(\{\boldsymbol{\Delta}_m\}) \propto \frac{\mathrm{e}^{-\frac{1}{3}q_0\ell N}}{\left(\sum_{m=1}^{M}\Delta_m\right)^{M-1}} \exp\left[-\frac{3}{2\ell^2 N}\left(\sum_{m=1}^{M}\Delta_m\right)^2\right]. \tag{25}$$

The probability distribution $\mathbb{P}(\{\boldsymbol{\Delta}_m\})$ is reminiscent of a normal Gaussian, but is in fact significantly different since both the exponent and the denominator contain the *modulus* of the tube segment vector $\boldsymbol{\Delta}_m$. From here onwards we shall no longer write a bar over the preferred s_m in (24), since all expressions will use it as a parameter, not a variable.

3.2. Rouse model with tube constraints

In section 2 we reviewed the basic Rouse dynamics for an end-constrained chain and a corresponding stress tensor for an ideal, phantom network. Following the ideas in section 3.1, we imagine each polymer strand to be confined within M tube-like regions. The axis or primitive path of a tube represents all the conformations that are accessible to a chain section between two entanglement constraints. In figure 2, we define the current model variables. Let n_m be the polymer segment at the 'exit' of tube segment m, so that $n_M = N$, for a chain with N polymer segments between two crosslinks and confined to M tube segments. If s_m is the number of monomer steps within a tube segment m, then $s_m = n_m - n_{m-1}$. The monomer segments have position vectors $\boldsymbol{r}_n(t)$ and the tube segments have position vectors $\boldsymbol{y}_m$:

$$\boldsymbol{y}_m(t) \equiv \boldsymbol{r}|_{n=n_m} = 2\sum_{p=1}^{N} \mathrm{x}_p(t) \sin\left[\frac{p\pi n_m}{N}\right]; \tag{26}$$

recall that the span vector of the mth tube segment is defined as $\boldsymbol{\Delta}_m = \boldsymbol{y}_m - \boldsymbol{y}_{m-1}$.

For this Rouse model of tube-constrained chains the stress tensor of a tube segment m, in the continuous limit, is given by

$$\sigma^{(m)}_{\alpha\beta}(t) = \frac{c}{N}k\int_0^{s_m} \mathrm{d}s \left\langle \frac{\partial r_{m\alpha}(s,t)}{\partial s}\frac{\partial r_{m\beta}(s,t)}{\partial s}\right\rangle_\psi , \tag{27}$$

where c again is the monomer density. This follows from (6), which gives the stress tensor of a single network strand between two crosslink points. As before, the notation $\langle\cdots\rangle_\psi$ denotes the time average of the components of stochastic force $\hat{\boldsymbol{f}}_p(t)$ over the distribution (7). Analogous to (3*a*), the position vector of a monomer (or bead) at the contour length s within the tube segment m, denoted by $\boldsymbol{r}_m(s,t)$, is written in terms of the span vector:

$$\boldsymbol{r}_m(s,t) = \boldsymbol{y}_{m-1} + \frac{s}{s_m}\boldsymbol{\Delta}_m + \boldsymbol{\rho}_m(t), \qquad \text{with} \quad \boldsymbol{\rho}_m(t) = 2\sum_{p=1}^{s_m} \mathrm{x}_p(t)\sin\left[\frac{p\pi s}{s_m}\right]. \tag{28}$$

Note that the 'loop' position vector $\boldsymbol{\rho}_m(t)$ has a shorter period now, so that $\boldsymbol{r}_m(s_m,t) - \boldsymbol{r}_m(0,t) = \boldsymbol{\Delta}_m$. In the phantom model of section 2.1, the equivalent boundary condition is given by $\boldsymbol{r}_N(t) - \boldsymbol{r}_0(t) = \boldsymbol{R}$. By summing $\sigma^{(m)}_{\alpha\beta}$ over M tube segments, one defines the microscopic stress tensor for a single chain between crosslinks:

$$\sigma^{(\mathrm{ch})}_{\alpha\beta}(t) = \frac{c}{N}\kappa\sum_{m=1}^{M}\int_0^{s_m} \mathrm{d}s \left\langle \frac{\partial r_{m\alpha}(s,t)}{\partial s}\frac{\partial r_{m\beta}(s,t)}{\partial s}\right\rangle_\psi , \tag{29}$$

which, by using (28), can be written in terms of normal coordinates and the span vectors, as follows:

$$\sigma^{(\mathrm{ch})}_{\alpha\beta}(t) = \frac{c}{N}\kappa\sum_{m=1}^{M}\left[\int_0^{s_m} \mathrm{d}s \left\langle \left(\frac{\Delta_{m\alpha}}{s_m} + \frac{\partial\rho_{m\alpha}}{\partial s}\right)\left(\frac{\Delta_{m\beta}}{s_m} + \frac{\partial\rho_{m\beta}}{\partial s}\right)\right\rangle_\psi\right] \tag{30a}$$

$$= \frac{c}{N}\kappa\sum_{m=1}^{M}\left[\frac{1}{s_m}\Delta_{m\alpha}\Delta_{m\beta} + \sum_{p=1}^{s_m}\frac{2\pi^2p^2}{s_m}\langle x_{p\alpha}(t)x_{p\beta}(t)\rangle_\psi\right] \tag{30b}$$

(the last line follows after integrating with respect to s). The first term is independent of s and of random noise. The last term survived the s-integration and still has to be averaged with respect to the thermal noise. Following the method outlined in section 2.2, the full solution of the Langevin equation is

$$x_{p\alpha}(t) = E_{\alpha\mu}x_{p\mu}(0^-)\,\mathrm{e}^{-t/\tilde{\tau}_p} + \frac{1}{\zeta_\mathrm{R}}\int_0^t \mathrm{e}^{-(t-t')/\tilde{\tau}_p}\hat{f}_{p\alpha}(t')\,\mathrm{d}t', \tag{31}$$

where the mode times are as before, $\tilde{\tau}_p = \tilde{\tau}_\mathrm{S}/p^2$, but with a shorter 'Rouse time' given by $\tilde{\tau}_\mathrm{S} \propto s_m^2/k_\mathrm{B}T$. Again, this is a diffusion problem for an effective 'particle' in a harmonic potential, but with a different constant

$$\tilde{k}_p = \frac{2\pi\kappa p^2}{s_m} = \frac{6\pi^2k_\mathrm{B}T}{s_m\ell^2}p^2 \qquad \text{and} \qquad \tilde{\tau}_p = \frac{\zeta s_m^2}{\pi^2\kappa p^2}. \tag{32}$$

Keeping in mind the change in the Rouse time and normal mode diffusion constant, the correlation function in (30*b*) is again given by (17), which now becomes

$$\langle x_{p\alpha}(t)x_{p\beta}(t)\rangle_\psi|_{t\to\infty} = \frac{k_\mathrm{B}T}{\tilde{k}_p}\delta_{\alpha\beta} = \frac{s_m\ell^2}{6\pi^2p^2}\delta_{\alpha\beta}. \tag{33}$$

The stress tensor of the whole network can be expressed as the ensemble average of $\sigma^{(\mathrm{ch})}_{\alpha\beta}$ over the quenched probability to find a given tube-confined strand with tube vectors described

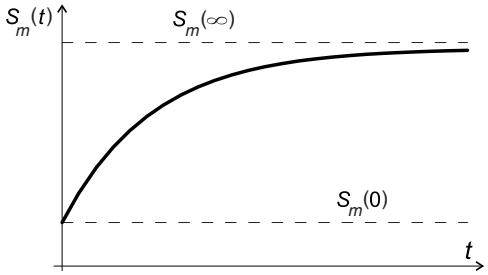

Figure 3. Illustrating the kinetic equation (35) for s_m.

by the set $\{\boldsymbol{\Delta}_m\}$. This probability is proportional to the total number of configurations of the whole crosslinked strand, given by $\mathbb{P}(\{\boldsymbol{\Delta}_m\})$ in (25). In the melt before crosslinking, the ensemble of chains obeys the distribution (25). The process of crosslinking not only quenches the end points of each strand, but also quenches the nodes of the primitive path $\boldsymbol{\Delta}_m$, since we assume the crosslinked chains cannot release the constraints by reptation. In our mean-field approach, the tube segments described by $\boldsymbol{\Delta}_m$ are conserved, although deformed by the strains applied to the network.

In this work we apply the affine deformation assumption with respect to the end-to-end vectors, denoted by $\boldsymbol{R}_0$. Since $\sum_{m=1}^{M} \boldsymbol{\Delta}_m = \boldsymbol{R}_0$, it follows that the span vectors deform affinely as well, that is, $\boldsymbol{\Delta}'_m = \boldsymbol{E} \cdot \boldsymbol{\Delta}_m$. Furthermore, any affine deformation $\boldsymbol{E}$ transforms the span vector lengths $\Delta_m = |\boldsymbol{\Delta}_m|$ into $\Delta'_m = |\boldsymbol{E} \cdot \boldsymbol{\Delta}_m|$, but leaves the quenched distribution $\mathbb{P}(\{\boldsymbol{\Delta}_m\})$ unchanged. Bearing this in mind, we can present the dynamic stress tensor of the crosslinked network in its most compact form:

$$\sigma_{\alpha\beta}(t) = \frac{c}{N}\kappa \sum_{m=1}^{M} \left[\!\!\left[\frac{[\boldsymbol{E}\cdot\boldsymbol{\Delta}_m]_\alpha [\boldsymbol{E}\cdot\boldsymbol{\Delta}_m]_\beta}{s_m(t)} + \sum_{p=1}^{s_m(t)} \frac{2\pi^2 p^2}{s_m(t)} \langle x_{p\alpha}(t) x_{p\beta}(t)\rangle \right]\!\!\right]_{\mathbb{P}(\{\boldsymbol{\Delta}_m\})}$$
$$\equiv \sigma^A_{\alpha\beta} + \sigma^B_{\alpha\beta}. \tag{34}$$

The brackets $[\![\cdots]\!]_{\mathbb{P}}$ refer to the quenched average with respect to the distribution $\mathbb{P}\{\boldsymbol{\Delta}_m\}$ proportional to the statistical weight given in (25).

The next step is to decide on the functional form of $s_m(t)$, as the number of segments in each tube is expected to change with time after the deformation is applied. As the mth tube vector $\boldsymbol{\Delta}_m$ transforms to $\boldsymbol{\Delta}'_m$, so does the number of polymer segments confined within this tube transform from $s_m(t=0)$ given by (24) to the final equilibrium value $s_m(t\to\infty)$ determined by the new $\boldsymbol{\Delta}'_m$. It is physically plausible to use a growth function of the form, cf figure 3,

$$s_m(t) = s_m(\infty)(1 - \mathrm{e}^{-\gamma t}) + s_m(0)\,\mathrm{e}^{-\gamma t}, \tag{35}$$

where the boundary values are given by

$$s_m(0) = \frac{N|\boldsymbol{\Delta}_m|}{\sum_{m'=1}^{M}|\boldsymbol{\Delta}_{m'}|} \qquad \text{and} \qquad s_m(\infty) = \frac{N|\boldsymbol{E}\cdot\boldsymbol{\Delta}_m|}{\sum_{m'=1}^{M}|\boldsymbol{E}\cdot\boldsymbol{\Delta}_{m'}|}. \tag{36}$$

3.3. Equilibrium limit

First, we calculate the equilibrium solution by taking the $t \to \infty$ limit in (34). Using the equilibrium limit of (35), we evaluate the two terms in the stress expression separately. The first part depends on the deformed span vectors as follows:

$$\sigma^A_{\alpha\beta}(t\to\infty) = \frac{c}{N}\kappa \left[\!\!\left[\sum_{m=1}^{M} \frac{\sum_{m'=1}^{M} |\boldsymbol{E}\cdot\boldsymbol{\Delta}_{m'}|}{N|\boldsymbol{E}\cdot\boldsymbol{\Delta}_m|} [\boldsymbol{E}\cdot\boldsymbol{\Delta}_m]_\alpha [\boldsymbol{E}\cdot\boldsymbol{\Delta}_m]_\beta \right]\!\!\right]_{\mathbb{P}(\{\boldsymbol{\Delta}_m\})}. \tag{37}$$

The second part follows from (33) and is given by

$$\sigma^B_{\alpha\beta}(t\to\infty) = \frac{c}{N}\kappa \left[\!\!\left[\sum_{m=1}^{M}\sum_{p=1}^{s_m} \frac{2\pi^2 p^2}{s_m}\frac{k_\mathrm{B}T}{\tilde{k}_p}\delta_{\alpha\beta} \right]\!\!\right] = \frac{c}{N}k_\mathrm{B}T \left[\!\!\left[\sum_{m=1}^{M}\sum_{p=1}^{s_m} \delta_{\alpha\beta} \right]\!\!\right]_{\mathbb{P}(\{\boldsymbol{\Delta}_m\})}. \tag{38}$$

Since $s_m(\infty)$ is given by (36), one has to substitute the Δ_m-dependent value into the sum *prior* to averaging with respect to $\mathbb{P}(\{\Delta_m\})$. Nevertheless, this term again gives the trivial result contributing only to the effective pressure:

$$\sigma^B_{\alpha\beta}(t\to\infty) = \frac{c}{N}k_\mathrm{B}T \left[\!\!\left[\sum_{m=1}^{M} \frac{N|\boldsymbol{E}\cdot\boldsymbol{\Delta}_m|}{\sum_{m'=1}^{M}|\boldsymbol{E}\cdot\boldsymbol{\Delta}_{m'}|}\delta_{\alpha\beta} \right]\!\!\right]_{\mathbb{P}(\{\boldsymbol{\Delta}_m\})} = \frac{c}{N}k_\mathrm{B}T N\delta_{\alpha\beta}. \tag{39}$$

We proceed to solve the main stress contribution in equilibrium, given by (37). Let us write span vectors as $\boldsymbol{\Delta}_m = \Delta_m \boldsymbol{e}_m$, with $\boldsymbol{e}_m$ being unit vectors of their orientation. The sums within the $[\![\cdots]\!]$ brackets can be factored as follows:

$$\sum_{m=1}^{M} \Delta_m^2 \,(\boldsymbol{E}\cdot\boldsymbol{e}_m)_\alpha\,(\boldsymbol{E}\cdot\boldsymbol{e}_m)_\beta + \sum_{\substack{m,m'=1\\ m\neq m'}}^{M} \Delta_m\Delta_{m'}|\boldsymbol{E}\cdot\boldsymbol{e}_{m'}|\frac{(\boldsymbol{E}\cdot\boldsymbol{e}_m)_\alpha\,(\boldsymbol{E}\cdot\boldsymbol{e}_m)_\beta}{|\boldsymbol{E}\cdot\boldsymbol{e}_m|}. \tag{40}$$

When averaging, the first part leads to M terms and the second to $M(M-1)$ terms; the stress becomes

$$\begin{aligned}\sigma^A_{\alpha\beta}(t\to\infty) = {}& \frac{c}{N}\kappa M [\![\Delta_m^2 (\boldsymbol{E}\cdot\boldsymbol{e}_m)_\alpha (\boldsymbol{E}\cdot\boldsymbol{e}_m)_\beta]\!] \\ & + \frac{c}{N}\kappa M(M-1)\left[\!\!\left[\Delta_m\Delta_{m'}\frac{|\boldsymbol{E}\cdot\boldsymbol{e}_{m'}|(\boldsymbol{E}\cdot\boldsymbol{e}_m)_\alpha(\boldsymbol{E}\cdot\boldsymbol{e}_m)_\beta}{|\boldsymbol{E}\cdot\boldsymbol{e}_m|}\right]\!\!\right].\end{aligned} \tag{41}$$

The procedure of evaluating the quenched averages of the form $[\![\Delta_m\Delta_{m'}]\!]$ with the probability distribution $\mathbb{P}(\{\boldsymbol{\Delta}_m\})$ given by (25) is given in the appendix. After completing the integration over the absolute values $|\boldsymbol{\Delta}_m|$ and simplifying all the front factors, including the normalization, the resulting stress expression takes the form

$$\begin{aligned}\sigma^A_{\alpha\beta}(\infty) = 4\frac{c}{N}k_\mathrm{B}T\frac{2M+1}{3M+1}\Bigg\{ & (4\pi)^{-1}\int \mathrm{d}\Omega_m (\boldsymbol{E}\cdot\boldsymbol{e}_m)_\alpha(\boldsymbol{E}\cdot\boldsymbol{e}_m)_\beta \\ & + (M-1)(4\pi)^{-2}\int \mathrm{d}\Omega_m \frac{(\boldsymbol{E}\cdot\boldsymbol{e}_m)_\alpha(\boldsymbol{E}\cdot\boldsymbol{e}_m)_\beta}{|\boldsymbol{E}\cdot\boldsymbol{e}_m|}\int \mathrm{d}\Omega_{m'}|\boldsymbol{E}\cdot\boldsymbol{e}_{m'}|\Bigg\}.\end{aligned} \tag{42}$$

Recall that $\tilde{c} = c/N$ is the average crosslink density of the system. The last step is to perform the remaining angular integrations over orientations $\boldsymbol{e}_m$. This depends on the particular geometry of deformation $\boldsymbol{E}$.

Let us first consider a small shear deformation given by

$$\boldsymbol{E} = \begin{pmatrix} 1 & \varepsilon & 0 \\ 0 & 1 & 0 \\ 0 & 0 & 1 \end{pmatrix} \quad \Rightarrow \quad \begin{aligned} (\boldsymbol{E}\cdot\boldsymbol{e}_m)_x &= \sin\theta_m(\cos\phi_m + \varepsilon\sin\phi_m) \\ (\boldsymbol{E}\cdot\boldsymbol{e}_m)_y &= \sin\theta_m\sin\phi_m \\ (\boldsymbol{E}\cdot\boldsymbol{e}_m)_z &= \cos\theta_m, \end{aligned} \tag{43}$$

where the notation used so far was rewritten in terms of spherical coordinates for the specific case of a shear deformation. We again refer the reader to the appendix for detailed calculations. From (A.11) and (A.12), the stress tensor (42) becomes

$$\sigma_{xy}(t \to \infty) = \frac{4}{3}\tilde{c}k_{\mathrm{B}}T\frac{2M+1}{3M+1}\left[1+\frac{4}{5}(M-1)\right]\varepsilon. \tag{44}$$

The approximately linear dependence of shear modulus on the entanglement number, in the limit $M \gg 1$, agrees with other approaches to equilibrium elasticity of entangled rubbers [17, 32, 33]. In the *phantom* limit (i.e. taking $M \to 1$) the equilibrium shear modulus returns to $G_0 = \sigma_{xy}/\varepsilon = \tilde{c}k_{\mathrm{B}}T$, as expected. In the strongly entangled limit, at $M \gg 1$, the shear modulus increases to $G \approx (32/45)M\tilde{c}k_{\mathrm{B}}T$.

Next, consider an arbitrary large uniaxial volume-preserving strain given by

$$\boldsymbol{E} = \begin{pmatrix} 1/\sqrt{\lambda} & 0 & 0 \\ 0 & 1/\sqrt{\lambda} & 0 \\ 0 & 0 & \lambda \end{pmatrix} \quad \Rightarrow \quad \begin{aligned} (\boldsymbol{E}\cdot\boldsymbol{e}_m)_x &= \lambda^{-1/2}\sin\theta_m\cos\phi_m \\ (\boldsymbol{E}\cdot\boldsymbol{e}_m)_y &= \lambda^{-1/2}\sin\theta_m\sin\phi_m \\ (\boldsymbol{E}\cdot\boldsymbol{e}_m)_z &= \lambda\cos\theta_m, \end{aligned} \tag{45}$$

where we again change to spherical coordinates to simplify integration. Substituting the results of the integrals (A.13) back into the stress tensor (42), we obtain the relevant stress components and therefore the tensile stress:

$$\begin{aligned} \sigma_{\mathrm{T}}(t \to \infty) &\equiv \sigma_{zz} - \sigma_{xx} \\ &= \tilde{c}k_{\mathrm{B}}T\frac{2M+1}{3M+1}\left\{\frac{4}{3}\left(\lambda^2 - \frac{1}{\lambda}\right) + (M-1)\left[\frac{(4\lambda^3-1)\arcsin^2\sqrt{1-\lambda^3}}{2\lambda(1-\lambda^3)^2}\right.\right. \\ &\quad \left.\left. - \frac{\sqrt{\lambda}\arcsin\sqrt{1-\lambda^3}}{\sqrt{1-\lambda^3}} - \frac{\lambda^2(1+2\lambda^3)}{2(1-\lambda^3)}\right]\right\}. \end{aligned} \tag{46}$$

By taking $\lambda \to 1+\varepsilon$, with $\varepsilon \ll 1$, one obtains the expression for the Young modulus from the linear tensile stress:

$$\sigma_{\mathrm{T}}(t \to \infty)|_{\lambda\to 1+\varepsilon} = \tilde{c}k_{\mathrm{B}}T\frac{4(2M+1)(4M+1)}{5(3M+1)}\varepsilon + \mathcal{O}[\varepsilon^2]. \tag{47}$$

It satisfying to note that the Young modulus $Y = \sigma_{\mathrm{T}}/\varepsilon$ is exactly three times the equilibrium shear modulus from (44), in spite of quite different and complicated integration route leading to each of the expressions.

3.4. Different dynamic regimes

In general, during the course of stress relaxation all the expressions depend on the kinetic function for the tube segment number $s_m(t)$, for which we have assumed the form (35), shown in figure 3. This makes $\mathbb{P}(\{\boldsymbol{\Delta}_m\})$ much more complicated, and we therefore only investigate certain cases here.

Case 1. Behaviour at $t \to 0$. For short time scales we expect the behaviour at the level of individual chain segments to be the same as for the phantom model of section 2.2, since the segments will not experience the effect of the tube constraints yet. Taking $t = 0$ and $s_m(t)$ as $s_m(0)$, the stress tensor (34) becomes

$$\sigma_{\alpha\beta}|_{t=0} = \tilde{c}\frac{\kappa}{N}\sum_{m,m'=1}^{M}[\![\Delta_m\Delta_{m'}[\boldsymbol{E}\cdot\boldsymbol{e}_m]_\alpha[\boldsymbol{E}\cdot\boldsymbol{e}_m]_\beta]\!]_{\mathbb{P}(\{\boldsymbol{\Delta}_m\})} + \tilde{c}k_{\mathrm{B}}TN(\boldsymbol{E}\boldsymbol{E}^{\top})_{\alpha\beta}. \tag{48}$$

The term in $[\![\cdots]\!]_{\mathbb{P}}$ brackets is averaged in the same way as before. For a uniaxial deformation, the tensile stress is given by

$$\sigma_{\mathrm{T}} = \sigma_{zz} - \sigma_{xx}|_{t=0} = \tilde{c}k_{\mathrm{B}}T\left(\lambda^2 - \frac{1}{\lambda}\right)\left[\frac{1}{3}(2M+1) + N\right], \tag{49}$$

and the resulting shear modulus at $t \to 0$ is

$$G = \tilde{c}k_{\mathrm{B}}T\left[\frac{1}{3}(2M+1) + N\right]. \tag{50}$$

In the limit of no entanglements ($M = 1$), one obtains the phantom result, $G = NG_0$, as expected.

Case 2. s_m equilibrates slowly. This is the situation when most of the time dependence is due to slow s_m-relaxations, that is, limited by the rate of redistribution of chain segments between the steps of primitive path after deformation. This is the limit when $\gamma \ll 1/\tau_p$ for all p, and so we can take $\mathrm{e}^{-t/\tau_p} \to 0$ in the Rouse sums. The stress tensor (34) becomes

$$\sigma_{\alpha\beta} = \tilde{c}\kappa\sum_{m=1}^{M}\left[\!\!\left[\frac{[\boldsymbol{E}\cdot\boldsymbol{\Delta}_m]_\alpha[\boldsymbol{E}\cdot\boldsymbol{\Delta}_m]_\beta}{s_m(\infty) - [s_m(\infty) - s_m(0)]\exp(-\gamma t)}\right]\!\!\right]_{\mathbb{P}(\{\boldsymbol{\Delta}_m\})} + \tilde{c}k_{\mathrm{B}}TN\delta_{\alpha\beta}. \tag{51}$$

This results in a difficult tube-span vector average, and we are forced to make a simplifying assumption that $\sum_n(|\boldsymbol{E}\cdot\boldsymbol{e}_n| - |\boldsymbol{E}\cdot\boldsymbol{e}_m|)\Delta_n \approx (1 - \boldsymbol{E}\cdot\boldsymbol{e}_m|)\sum_n \Delta_n$, such that we obtain a more tractable expression to average. We have

$$\sigma_{\alpha\beta} \approx \tilde{c}\frac{\kappa}{N}\sum_{m=1}^{M}\left[\!\!\left[\frac{\Delta_m[\boldsymbol{E}\cdot\boldsymbol{e}_m]_\alpha[\boldsymbol{E}\cdot\boldsymbol{e}_m]_\beta\sum_n\Delta_n|\boldsymbol{E}\cdot\boldsymbol{e}_n|}{(1-|\boldsymbol{E}\cdot\boldsymbol{e}_m|)\exp(-\gamma t) + |\boldsymbol{E}\cdot\boldsymbol{e}_m|}\right]\!\!\right]_{\mathbb{P}(\{\boldsymbol{\Delta}_m\})} + \tilde{c}k_{\mathrm{B}}TN\delta_{\alpha\beta}, \tag{52}$$

where the effective pressure correction in the last term will be dropped from now on Following the same method for averaging the tube vector spans $|\boldsymbol{\Delta}_m|$, we end up with the following deformation-dependent expression:

$$\sigma_{\alpha\beta} = 4\tilde{c}k_{\mathrm{B}}T\frac{2M+1}{3M+1}\left\{(4\pi)^{-1}\int \mathrm{d}\Omega_m \frac{(\boldsymbol{E}\cdot\boldsymbol{e}_m)_\alpha(\boldsymbol{E}\cdot\boldsymbol{e}_m)_\beta}{1 + (|\boldsymbol{E}\cdot\boldsymbol{e}_m|^{-1} - 1)\,\mathrm{e}^{-\gamma t}}\right.$$
$$\left. + \frac{(M-1)}{(4\pi)^2}\int \mathrm{d}\Omega_m \frac{(\boldsymbol{E}\cdot\boldsymbol{e}_m)_\alpha(\boldsymbol{E}\cdot\boldsymbol{e}_m)_\beta}{|\boldsymbol{E}\cdot\boldsymbol{e}_m|\{1 + (|\boldsymbol{E}\cdot\boldsymbol{e}_m|^{-1} - 1)\,\mathrm{e}^{-\gamma t}\}}\int \mathrm{d}\Omega_{m'}|\boldsymbol{E}\cdot\boldsymbol{e}_{m'}|\right\}. \tag{53}$$

In the case of small shear deformation, as in section 3.3, the shear modulus near the equilibrium takes the form

$$G(t) = \frac{4}{15}\tilde{c}k_{\mathrm{B}}T\frac{2M+1}{3M+1}(1 + 4M + M\,\mathrm{e}^{-\gamma t}), \tag{54}$$

which now includes a new relaxation time $1/\gamma$ (recall $\gamma\tau_p \ll 1$ in this regime), and gives the correct result in the $M = 1$ limit of a phantom network in equilibrium.

Case 3. s_m equilibrates fast. This is the opposite case, corresponding to the situation when the reptation of chain segments between different tubes of the primitive path is fast and the value $s_m(\infty)$ is reached before the majority of the Rouse modes had time to dissipate. In other words, this is the limit of $\gamma\tau_p \gg 1$ for all or most p. The result may be expected to be trivial: a combination of the new equilibrium plateau result given by (47) and the old Rouse behaviour interpolating between $G(t=0) \approx N\tilde{c}k_{\mathrm{B}}T$ and $G(t) \sim t^{-1/2}$. Indeed, the first part

of the stress tensor is identical to the equilibrium case, cf σ^A in (34) and (37). However, the second part, denoted by σ^B in (34), is more difficult to treat. To simplify the calculations, the shear modulus $G(t)$ can be inspected for different time regimes, written in terms of the defined Rouse times:

$$G(t) \approx G_{\mathrm{eq}} + \begin{cases} G_0 \sum_{m=1}^{M} [\![\mathrm{e}^{-2t/\tilde{\tau}_{\mathrm{S}}}]\!]_{\mathbb{P}(\{\boldsymbol{\Delta}_m\})} & t \gg \frac{\zeta s_m^2}{\pi^2 \kappa} \equiv \tilde{\tau}_{\mathrm{S}} \\ \frac{1}{2} G_0 N \sqrt{\frac{\zeta}{2\pi\kappa}} t^{-1/2} & t \sim \tilde{\tau}_{\mathrm{S}} \\ G_0 \sum_{m=1}^{M} \left[\!\!\left[\sum_{p=1}^{s_m} \mathrm{e}^{-2tp^2/\tilde{\tau}_{\mathrm{S}}} \right]\!\!\right]_{\mathbb{P}(\{\boldsymbol{\Delta}_m\})} & \tilde{\tau}_{\mathrm{S}} > t > \tilde{\tau}_p \\ G_0 (N + M\, \mathrm{e}^{-2\pi^2 \kappa t/\zeta}) & t \ll \frac{\zeta}{\pi^2 \kappa} = \tilde{\tau}_{\mathrm{S}}/s_m^2. \end{cases} \tag{55}$$

Only half of the above cases have closed-form solutions. The remaining cases, indicated by the presence of $[\![\cdots]\!]$ brackets, will need more severe assumptions or a direct numerical approach.

Case 4. Mean-field average for s_m. We can obtain a very crude estimate of the dynamic stress tensor by making an assumption that the number of chain segments in each tube equilibrates first (as in case 3), and also that there is on average the same number of segments in each tube: $\bar{s}_m^* = N/M$. Such an assumption can only realistically be defended if $M \gg 1$ and all tube sections are relatively short, with narrow distribution. However, we can make an easy analytical progress, since the main difficulty of this problem (in determining $\bar{s}_m(t, \lambda)$) is removed. In this case, the longest Rouse mode $\tilde{\tau}_{\mathrm{S}}^* = \zeta N^2/(\pi^2 \kappa M^2) = \tau_{\mathrm{R}}/M^2$ and the stress tensor (34) simplifies greatly:

$$\begin{aligned} \sigma_{\alpha\beta}(t) = \tilde{c}\kappa \frac{M}{N} \sum_{m=1}^{M} [\![\Delta_m^2 [\boldsymbol{E} \cdot \boldsymbol{e}_m]_\alpha [\boldsymbol{E} \cdot \boldsymbol{e}_m]_\beta]\!]_{\mathbb{P}(\{\boldsymbol{\Delta}_m\})} \\ + \tilde{c} k_{\mathrm{B}} T \sum_{m=1}^{M} \sum_{p=1}^{N/M} [(\boldsymbol{E}\boldsymbol{E}^{\top})_{\alpha\beta}\, \mathrm{e}^{-2tp^2/\tilde{\tau}_{\mathrm{S}}} + (1 - \mathrm{e}^{-2tp^2/\tilde{\tau}_{\mathrm{S}}^*}) \delta_{\alpha\beta}]. \end{aligned} \tag{56}$$

After the integration with respect to $\mathbb{P}$, the tensile stress takes the form

$$\sigma_{\mathrm{T}} = \tilde{c} k_{\mathrm{B}} T M \left\{ \frac{4}{3} \frac{(2M+1)}{(3M+1)} + \sum_{p=1}^{N/M} \exp\left(\frac{-2tp^2}{\tilde{\tau}_{\mathrm{S}}^*} \right) \right\} \left(\lambda^2 - \frac{1}{\lambda} \right). \tag{57}$$

This expression gives consistent results for the shear modulus in both the equilibrium and $t = 0$ limits, and shows the characteristic $t^{-1/2}$ transition between these regimes.

4. Summary

We have presented an improved stress-based model of polymer network dynamics, which combines both the traditional rubber network elasticity and the Rouse approach to dynamics and relaxation. In this model, we have assumed the crosslinks to be spatially fixed and to deform affinely. This is clearly a weakness, characteristic of many rubber-elasticity treatments. Experiments have shown that network deformations at a microscopic length scale are not always affine [34, 35], and there are several theories that begin to address this complication in equilibrium [36]. However, in our dynamical treatment we are not able to raise the traditional affine approximation. In the same way, complications due to finite extensibility of chains at large deformations and network defects (loops and dangling ends) are not taken into account, while we develop a dynamical formalism.

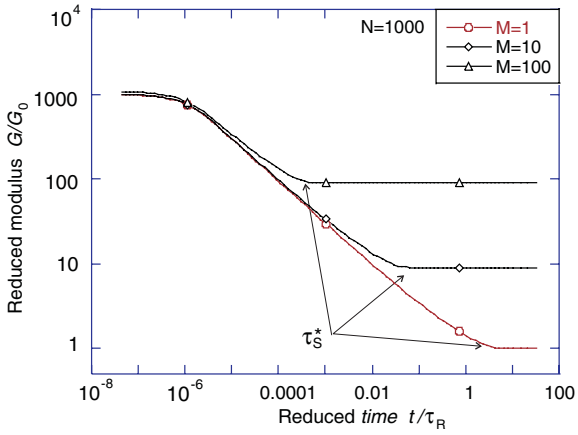

Figure 4. Plotting the equation (57): $G(t)/G_0$ against t/τ_R (the original Rouse time), for different vales of M. The slope of the power-law decay is -0.5, in agreement with the underlying Rouse ideas and the corresponding limit in (55). The nominal glass transition occurs at $t \ll \tau_R/N^2$, with G given by (50). At $t \gg \tau_S^*$ the equilibrium modulus approaches the value given by (44).

In section 2 we review an improved stress–tensor model, where both force and position boundary conditions at the crosslinked endpoints of the flexible phantom chains were rigorously enforced. Previously [18], only the position boundary conditions were observed, resulting in an effective 'tethered-chain network'. The results in section 2.2 provide a smooth crossover in accounting for the dynamical behaviour spanning all timescales. The aim of this paper was to describe entangled systems, which show qualitatively different dynamic-mechanical responses from the earlier phantom model. In section 3, we used the mean-field tube approach and obtained a general expression for the dynamic stress tensor. From this tensor, we obtain the equilibrium response for a tube-confined network. It is somewhat different from other expressions accounting for equilibrium elasticity of entangled rubbers, but has the same qualitative features. Lastly, we investigated the general dynamic stress tensor in four different limiting cases: at $t \to 0$ ('glassy' response immediately after applying step strain), the case of slow s_m-equilibration, fast *tube*-equilibration and an approximation when s_m equilibrates at a single mean value for each tube segment. To improve this theory further, we need either a different kinetic equation for $s_m(t)$ evolution or a numerical approach for the cases where a closed-form solution is not attainable.

In this paper we only work with a dry polymer system (with no solvent effects), aiming at understanding the basic principles of combined network and tube constraints. However, an extension to swollen gels is possible and should be quite straightforward—for example, the key parameter M has been estimated as $M \propto \phi^{-4/3}$, with ϕ the polymer volume fraction [37, 38]. The strength of our formulation is in its generalization of the Doi–Edwards tube formulation for entangled networks where it offers the possibility of an analytic expression for $G(t)$.

Acknowledgments

We are grateful for many discussions with James Adams, Yong Mao and Peter Olmsted. This research has been supported by EPSRC via the TCM/CUC3 Portfolio partnership.

Appendix

In order to evaluate the thermodynamic averages of the form $[\![\Delta_m \Delta_{m'}]\!]$ of section 3.3, one needs to average $\Delta_m \Delta_{m'} = |\boldsymbol{\Delta}_m||\boldsymbol{\Delta}_{m'}|$ with the probability distribution $\mathbb{P}(\{\boldsymbol{\Delta}_m\})$ given by (25). This is done in three steps: calculate the normalization factor, calculate the averages over the moduli $\{\Delta_m\}$ and lastly over the orientation vectors $\{\boldsymbol{e}_m\}$.

A.1. The normalization factor

The normalization factor $\mathcal{N}$ of the distribution is calculated by introducing a new scalar variable $u = \sum_{m=1}^{M} \Delta_m$ to simplify the exponent of the distribution

$$\mathcal{N} = \prod_{m=1}^{M} \int \mathrm{d}\boldsymbol{\Delta}_m \frac{\exp\left[-\frac{3}{2\ell^2 N}\left(\sum_{m=1}^{M} \Delta_m\right)^2\right]}{\left(\sum \Delta_m\right)^{M-1}} \tag{A.1}$$

$$= \prod_{m=1}^{M} \int \mathrm{d}\boldsymbol{\Delta}_m \int_0^\infty \mathrm{d}u\, \delta\left(u - \sum_{m=1}^{M} \Delta_m\right) \mathrm{e}^{-\frac{3}{2\ell^2 N}u^2} u^{-(M-1)} \tag{A.2}$$

$$= (4\pi)^M \int_0^\infty \mathrm{d}u \exp\left(-\frac{3}{2\ell^2 N}u^2\right) u^{-(M-1)} I_M(u), \tag{A.3}$$

where I_M is a function of u defined as follows:

$$I_M = \int_0^u \mathrm{d}\Delta_1 \Delta_1^2 \int_0^{u-\Delta_1} \mathrm{d}\Delta_2 \Delta_2^2 \ldots \int_0^{u-\cdots-\Delta_{M-2}} \mathrm{d}\Delta_{M-1} \Delta_{M-1}^2 \left(u - \sum_{i=1}^{M-1} \Delta_i\right)^2.$$

The distribution and the moduli Δ_m are invariant under rotations of the vectors $\boldsymbol{\Delta}_m$, so that the angular integration is done trivially by introducing spherical coordinates. Moreover, we implement the constraint $u = \sum \Delta_m$, and note that the moduli Δ_m cannot be negative. Since the integrals only involve power functions the function $I_M(u)$ is itself a power of u, whose order is determined by counting the dimensions:

$$I_M(u) = \frac{1}{X_m} u^{3M-1}. \tag{A.4}$$

Using this definition of the integral function, one can find a recursive relation

$$I_{M+1}(u) = \int_0^u \mathrm{d}\Delta_1 \Delta_1^2 I_M(u - \Delta_1) = \frac{2}{3M(3M+1)(3M+2)} \frac{u^{3(M+1)-1}}{X_M}, \tag{A.5}$$

and applying (A.4) to this relation and using the initial condition, $I_1 = u^2$, one can obtain all the coefficients X_M recursively:

$$X_{M+1} = \tfrac{1}{2} 3M(3M+1)(3M+2) X_M, \tag{A.6}$$

and thus all the functions $I_m(u)$ are known. Lastly, one performs a standard Gaussian integration over u to obtain the normalization:

$$\mathcal{N} = (4\pi)^M \frac{1}{2} \left(\frac{2\ell^2 N}{3}\right)^{M+\frac{1}{2}} \Gamma\left(M + \frac{1}{2}\right) \left[\prod_{\mathrm{i}=1}^{M-1} \frac{3\mathrm{i}}{2}(3\mathrm{i}+1)(3\mathrm{i}+2)\right]^{-1}. \tag{A.7}$$

A.2. Averaging the tube segment lengths $\{\Delta_m\}$

Having obtained the normalization constant $\mathcal{N}$, we can proceed to calculate the averages in (41). The calculations are similar to the above one for $\mathcal{N}$, but with more involved angular integrations, denoted by $\mathrm{d}\Omega$:

$$\sigma^A_{\alpha\beta}(\infty) = \frac{c}{N}\frac{\kappa M}{\mathcal{N}}\int_0^\infty \mathrm{d}u \exp\left(-\frac{3}{2\ell^2 N}u^2\right) u^{-(M-1)}\widetilde{I}_M(u)\left(\prod_{\tilde{m}=1}^{M}\int_{|e|=1}\mathrm{d}\Omega_{\tilde{m}}\right)$$
$$\times\left\{(\boldsymbol{E}\cdot\boldsymbol{e}_m)_\alpha\,(\boldsymbol{E}\cdot\boldsymbol{e}_m)_\beta + (M-1)\frac{|\boldsymbol{E}\cdot\boldsymbol{e}_{m'}|\,(\boldsymbol{E}\cdot\boldsymbol{e}_m)_\alpha\,(\boldsymbol{E}\cdot\boldsymbol{e}_m)_\beta}{|\boldsymbol{E}\cdot\boldsymbol{e}_m|}\right\}. \tag{A.8}$$

Again, we wrote each tube segment span vector as a product of its modulus, Δ_m, and its arbitrary orientation, denoted by the unit vector $\boldsymbol{e}_m$. The integrations over the moduli now include two more powers from Δ_m^2 and $\Delta_m\Delta_{m'}$ and counting the dimensions we obtain a slightly different recursive function to the one given in (A.4):

$$\widetilde{I}_M(u) = \frac{1}{\widetilde{X}_m}u^{3M+1}. \tag{A.9}$$

Repeating the same procedure as in (A.5), we obtain a recursive formula for the coefficients

$$\widetilde{X}_{M+1} = \tfrac{1}{2}(3M+2)(3M+3)(3M+4)\widetilde{X}_M. \tag{A.10}$$

After completing the moduli integrations (over Δ_m and u) and simplifying all the front factors, including the normalization factor, the stress expression only contains orientational integrals, cf (42).

A.3. Averaging the orientation vectors $\{\boldsymbol{e}_m\}$

The last step is to perform the remaining angular integrations. However, this is dependent on the *type* of deformation. First we consider a small shear deformation. From (43), it follows that

$$\int \mathrm{d}\Omega_m \frac{(\boldsymbol{E}\cdot\boldsymbol{e}_m)_x(\boldsymbol{E}\cdot\boldsymbol{e}_m)_y}{|\boldsymbol{E}\cdot\boldsymbol{e}_m|}$$
$$= \int_0^{2\pi}\mathrm{d}\phi_m\int_0^{\pi}\mathrm{d}\theta_m \frac{\sin^3\theta_m(\cos\theta_m\sin\phi_m + \varepsilon\sin^2\phi_m)}{[\sin^2\theta_m(1+2\varepsilon\cos\phi_m\sin\phi_m+\varepsilon^2\sin^2\phi_m)+\cos^2\theta_m]^{1/2}}$$
$$\approx \frac{16\pi}{15}\varepsilon \qquad \text{for} \quad \varepsilon \ll 1. \tag{A.11}$$

Similarly, for a *small* shear, the rest of the non-trivial angular integrations simplify:

$$\int \mathrm{d}\Omega_m|\boldsymbol{E}\cdot\boldsymbol{e}_m| \approx 4\pi \qquad \text{for} \quad \varepsilon \ll 1,$$
$$\int \mathrm{d}\Omega_m\,(\boldsymbol{E}\cdot\boldsymbol{e}_m)_x\,(\boldsymbol{E}\cdot\boldsymbol{e}_m)_y \approx \frac{4\pi}{3}\varepsilon \qquad \text{for} \quad \varepsilon \ll 1, \tag{A.12}$$

Next we consider a uniaxial deformation given by (47). This time we do not Taylor expand at all, but calculate the integrals exactly. This is possible since the deformation is a

diagonal matrix. The relevant integrals are listed below:

$$\int \mathrm{d}\Omega_m \frac{(\boldsymbol{E}\cdot\boldsymbol{e}_m)_x\,(\boldsymbol{E}\cdot\boldsymbol{e}_m)_x}{|\boldsymbol{E}\cdot\boldsymbol{e}_m|} = \int_0^{2\pi} \mathrm{d}\phi_m \int_0^{\pi} \mathrm{d}\theta_m \frac{1}{\lambda} \frac{\sin^3\theta_m \cos^2\phi_m}{\left[\frac{1}{\lambda}\sin^2\theta_m + \lambda^2\cos^2\theta_m\right]^{1/2}}$$

$$= 4\pi \left\{ \frac{2\lambda^3 - 1}{\lambda^{\frac{1}{2}}(\lambda^3-1)^{3/2}} \sinh^{-1}[\sqrt{\lambda^3 - 1}] - \frac{\lambda}{4(\lambda^3-1)} \right\},$$

$$\int \mathrm{d}\Omega_m \frac{(\boldsymbol{E}\cdot\boldsymbol{e}_m)_z\,(\boldsymbol{E}\cdot\boldsymbol{e}_m)_z}{|\boldsymbol{E}\cdot\boldsymbol{e}_m|} = 4\pi \left\{ \frac{\lambda^4}{2(\lambda^3-1)} - \frac{\lambda^{5/2}\sinh^{-1}[\sqrt{\lambda^3-1}]}{2(\lambda^3-1)^{3/2}} \right\},$$

$$\int \mathrm{d}\Omega_m |\boldsymbol{E}\cdot\boldsymbol{e}_m| = 4\pi \left(\frac{1}{2}\lambda + \frac{\sinh^{-1}[\sqrt{\lambda^3-1}]}{2\lambda^{1/2}\sqrt{\lambda^3-1}} \right),$$

$$\int \mathrm{d}\Omega_m (\boldsymbol{E}\cdot\boldsymbol{e}_m)_x (\boldsymbol{E}\cdot\boldsymbol{e}_m)_x = \frac{4\pi}{3}\frac{1}{\lambda}, \qquad \int \mathrm{d}\Omega_m (\boldsymbol{E}\cdot\boldsymbol{e}_m)_z (\boldsymbol{E}\cdot\boldsymbol{e}_m)_z = \frac{4\pi}{3}\lambda^2. \tag{A.13}$$

References

[1] Kuhn W 1934 *Kolloid Z.* **68** 2
[2] Ball R C, Edwards S F, Doi M and Warner M 1981 *Polymer* **22** 1010–18
[3] Edwards S F and Vilgis T A 1988 *Rep. Prog. Phys.* **51** 243–97
[4] Mergell B and Everaers R 2001 *Macromolecules* **34** 5675–86
[5] Rubinstein M and Panyukov S 2002 *Macromolecules* **35** 6670–86
[6] Xing X, Goldbart P M and Radzihovsky L 2007 *Phys. Rev. Lett.* **98** 075502
[7] Edwards S F and Doi M 1986 *The Theory of Polymer Dynamics* (Oxford: Clarendon)
[8] Mead D W, Larson R G and Doi M 1998 *Macromolecules* **31** 7895–914
[9] McLeish T C B 2002 *Adv. Phys.* **51** 1379–527
[10] Watanabe H 1999 *Prog. Polym. Sci.* **24** 1253–403
[11] Roberts A D 1988 *Natural Rubber Science and Technology* (Oxford: Clarendon)
[12] Edwards S F 1967 *Proc. Phys. Soc.* **91** 513–9
[13] De Gennes P G 1971 *J. Chem. Phys.* **55** 572–9
[14] Edwards S F and Doi M 1978 *J. Chem. Soc.: Faraday Trans. II* **74** 1789–802
[15] Flory P J 1969 *Principles of Polymer Chemistry* (New York: Interscience)
[16] Edwards S F 1974 *J. Phys. A: Math. Nucl. Gen.* **7** 318–31
[17] Edwards S F, Takano H and Terentjev E M 2000 *J. Chem. Phys.* **113** 5531
[18] Vandoolaeghe W L and Terentjev E M 2005 *J. Chem. Phys.* **123** 034902
[19] Adams J M, Mao Y and Vandoolaeghe W L 2007 *J. Chem. Phys.* **127** 114907
[20] Kutter S 2002 *PhD Thesis* University of Cambridge
[21] Graham R S, Likhtman A E, McLeish T C B and Milner S T 2003 *J. Rheol.* **47** 1171–200
[22] Mooney M 1959 *J. Polym. Sci.* **304** 599–626
[23] Marciano Y and Brochard-Wyart F 1995 *Macromolecules* **28** 985–90
[24] Quake S, Babcock H and Chu S 1997 *Nature* **388** 151–4
[25] Tang H 1996 *Macromolecules* **29** 2633–40
[26] Vandoolaeghe W L, Kutter S and Terentjev E M 2006 *J. Pol. Sci. B: Pol. Phys.* **44** 2679–97
[27] Treloar L R G 1975 *The Physics of Rubber Elasticity* (Oxford: Clarendon)
[28] Warner M and Terentjev E M 2003 *Liquid Crystal Elastomers* (Oxford: Oxford University Press)
[29] Terentjev E M, Hotta A, Clarke S M and Warner M 2003 *Phil. Trans. R. Soc. Lond.* A **361** 653
[30] Edwards S F 1977 *Br. Polym. J.* **6** 140–3
[31] Marucci G and Grizzuti N 1988 *Gazz. Chim. Ital.* **118** 179–85
[32] Ball R C, Doi M, Edwards S F and Warner M 1981 *Polymer* **22** 1010
[33] Higgs P G and Ball R C 1989 *Europhys. Lett.* **8** 357

[34] Bastide J and Leibler L 1988 *Macromolecules* **21** 2647
[35] Westermann S, Pyckout-Hintzen W, Richter D, Straube E, Egelhaaf S and May R 2001 *Macromolecules* **34** 2186
[36] Rabin Y and Panyukov S 1997 *Macromolecules* **30** 301
[37] Colby R H and Rubinstein M 1990 *Macromolecules* **23** 2753–60
[38] Milner S T and McLeish T C B 1998 *Phys. Rev. Lett.* **81** 725–28